Hindawi
Mathematical Problems in Engineering
Volume 2020, Article ID 2371059, 13 pages
https://doi.org/10.1155/2020/2371059

Research Article

Simulation and Experimental Study on Fishing Performance of Vacuum Suction Wellbore Cleaning Tool

Lei Qinglong,[1] **Wang Xueqiang**,[2] **Tang Geng**,[3] **Dong Liangliang**,[1] **Liao Yun**,[2] **Feng Xingzheng**,[2] **and Yang Yongtao**[2]

[1]*School of Mechatronic Engineering, Southwest Petroleum University, Chengdu, China*
[2]*Sichuan Shengnuo Oil and Gas Engineering Technology Services Co., Ltd., Chengdu, China*
[3]*Southwest Oil and Gas Field Company Engineering and Technology Research Institute, Chengdu, China*

Correspondence should be addressed to Lei Qinglong; leiqinglong@stu.swpu.edu.cn

Received 11 February 2020; Accepted 11 June 2020; Published 14 July 2020

Academic Editor: Daniel Zaldivar

During the completion of shale gas wells, bridge plug debris and debris particles are often left at the bottom of the well, which are difficult to clean up, pose a serious risk to wellbore operations, and reduce productivity. In order to solve the difficulty of cleaning the debris at the bottom of the well, a kind of wellbore cleaning tool is proposed based on the principle of negative jet pressure and liquid-solid two-phase flow theory. The finite element analysis method and laboratory test were used to verify the function of cleaning tools: the finite element method can effectively reflect the principle and process of dredging bottom debris with cleaning tools. In order to improve the applicability and fishing ability of wellbore cleaning tools, factors influencing the performance of cleaning tools were analyzed as follows: choosing high-density and low-viscosity working fluid is beneficial to improve the negative pressure effect of cleaning tools. Under the conditions of wellbore safety and economy, increasing pump pressure and displacement and reducing annular pressure can effectively increase the fishing performance of cleaning tools.

1. Introduction

As a cleaner and more efficient source of energy, shale gas could effectively reduce reliance on highly polluting fuels such as coal and oil [1]. In North America, shale gas extraction has been developed and commercialized [2]. Chinese government has also called for energy diversification, especially from shale gas. Shale gas production is expected to reach 3×10^{10} m^3 and 1×10^{11} m^3 in 2020 and 2030, respectively [3]. Shale substrates have low porosity and permeability and high flow resistance and often require horizontal wells and large-scale fracturing to achieve large-scale production [4]. However, when the bridge plug is used as a staging tool for pressure operation, the subsequent drill-back is not complete, and debris of the bridge plug will remain in the wellbore. The recovered bridge plug fragment is shown in Figure 1. Fracturing proppant backflow, sand, cuttings, and even shale debris are common after wellbore fracturing. Debris will accumulate in the horizontal section, while upwarped wells will accumulate near the lowest point, resulting in the failure of several wells to lower the completion tubing at a later stage, which will affect the production at a later stage [5]. If these residues are not removed in a timely manner, they will deposit continuously in the wellbore, which may lead to high torque, high resistance, stuck drilling, and other risks during the operation [6, 7]. In the completion process, the wellbore and surface production process may be blocked, which will greatly affect the gas well production [8]. A schematic diagram of formation plugging is shown in Figure 2.

To solve the wellbore cleaning problem, the most common method is sand washing operation, using the drilling fluid circulation to bring out the bottom debris [5]. However, this method has low cleaning efficiency and easily causes sticking when applied to horizontal wells [9, 10]. Therefore, for the problem of poor rock carrying effect, Bashir [7], Ozbayoglu et al. [11], Duane et al. [12],

Figure 1: Bridge plug fragment.

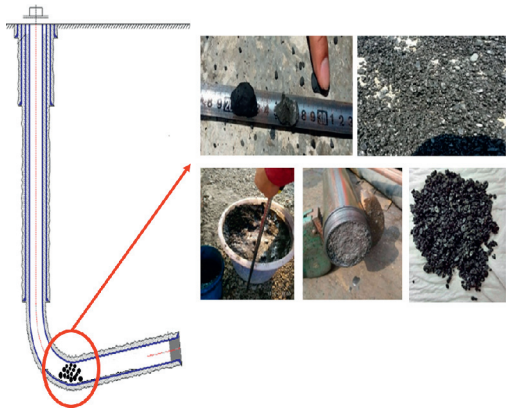

Figure 2: Formation blockage.

Han et al. [13], and Tie et al. [14] used a special downhole device to generate eddies to improve the fluid's ability to transport particles. However, when the sediment particles at the bottom of the well are large, they cannot be carried out of the well head. In addition, when the shale gas well enters the later stage of development, the reservoir pressure coefficient is low, or the wellbore itself is a carbonate fissure and cave-type formation, so not only the shaft wall is prone to collapse, but also the bottom of the well is prone to serious leakage, so the whole wellbore circulation cannot be established. As a result, sand washing technology is still difficult to achieve the need for bottom-hole cleaning of unconventional gas such as shale gas.

In order to solve the problem of poor cleaning effect of bottom hole impurities in oil and gas wells, a new type of bottom hole cleaning tool has been developed rapidly in recent years. The bottom hole cleaning tool uses high pressure water jet to generate local negative pressure in the interior, which can not only suck the straw string to sink sand but also capture small pieces of debris, so as to achieve the effect of cleaning the bottom hole impurities. The salvage process is shown in Figure 3. In this process, only local reverse circulation can be established near the tool to salvage the debris in the well [15, 16].

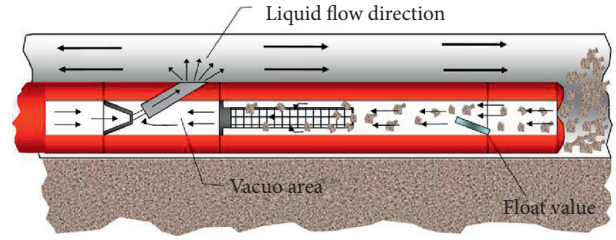

Figure 3: Schematic diagram of cleaning tool salvage.

The negative pressure effect of high-pressure water jet is widely used in other industries. The effects of different injection angles and different jet momentum on the concentration of the two mixtures were studied in the literature, such as Paterson [17], Eckerle et al. [18], and Sundararaj and Selladurai [19]. Boersma et al. [20] predicted the turbulence intensity, pressure, and mixing concentration in the jet. Eames et al. [21] and Kanjanapon and Satha [22] applied the negative pressure effect to the cooling system. Raman and Taghavi [23], Smith and Mungal [24], Sherif and Pletcher [25], and Said et al. [26] divided the process of high-pressure water jet into three stages, unmixed zone, mixed zone, and mixed stable zone, to better describe the suction phenomenon of negative pressure effect. David et al. [27] verified the ejector with negative pressure effect experimentally. However, the application of negative pressure effect to bottom hole cleaning tools is rarely studied, and the process of cleaning tools to salvage bottom hole impurities is not yet well understood.

In order to solve the problem of shaft cleaning in horizontal wells, this paper first proposes a wellbore cleaning tool based on the principle of negative jet pressure and liquid-solid two-phase flow theory. Then, the numerical model of scavenging tool for cuttings at the bottom of the well was carried out by using limited analysis method, and the mechanism of scavenging tool was tested in laboratory to verify the feasibility of scavenging tool. Finally, in order to ensure the maximum cleaning performance of the tool, the influence factors and operating parameters of the cleaning tool were analyzed and discussed using the finite element method, so as to determine the best operating conditions and operating parameters of the cleaning tool.

2. Cleaning Tool Verification

2.1. Cleaning Tool Salvage Verification

2.1.1. Cleaning Tool Principle. According to Bernoulli's equation, the incompressible fluid between the front and back of the nozzle can be described as [28, 29]

$$\frac{P_1}{\rho} + \frac{v_1^2}{2} = \frac{P_2}{\rho} + \frac{v_2^2}{2} + \zeta_1 \cdot \frac{v_2^2}{2}, \tag{1}$$

where P_1 and P_2 are the fluid pressure before and after the nozzle; v_1 and v_2 are the fluid velocity before and after the nozzle. ρ is the fluid density. $\xi 1$ is related to the friction coefficient, number, and shape of the nozzles and Reynolds number.

Therefore, the pressure difference before and after touching the mouth is

$$\Delta P = P_1 - P_2 = \frac{\rho}{2}\left(V_2^2 - V_1^2\right) + \zeta_1 \cdot \frac{\rho v_2^2}{2}, \tag{2}$$

where ΔP is the pressure difference before and after touching the mouth.

Since the nozzle is convergent, the area of the passing flow surface after the nozzle exits is much smaller than the inlet of the nozzle; therefore, $v_1 \ll v_2$, $\Delta P > 0$. The pressure drop at the nozzle outlet is obvious, which makes the liquid under the nozzle move upward under the action of pressure gradient and establishes local reverse circulation in the cleaning tool section.

The flow of bottom hole debris with the fluid belongs to solid-liquid two-phase flow, and the characteristic function of the debris can be expressed as

$$f = f(r, u, T, a, t), \tag{3}$$

where r is the spatial position, u is the particle velocity, T is the temperature, a is the particle radius, and t is the function with time.

The number of particles falling in the region of velocity $u - u + \mathrm{d}u$, temperature $T - T + \mathrm{d}T$, and radius $a - a + \mathrm{d}a$ is

$$d_n = f(r, u, T, a, t)\mathrm{d}r\,\mathrm{d}u\,\mathrm{d}\theta\,\mathrm{d}a. \tag{4}$$

The distribution function f is determined by the Boltzmann equation:

$$\frac{\partial f}{\partial t} + \frac{\partial}{\partial r}(uf) + \frac{\partial}{\partial r}(bf) + \frac{\partial}{\partial T}\left(\frac{Qf}{mC}\right) + \frac{\partial}{\partial T}\left(\frac{Mf}{3mk}\right) = \left(\frac{\partial f}{\partial t}\right)_c, \tag{5}$$

where b is the external force per unit mass received by a single particle, m is the mass of a single particle, Q is the heat conductivity of single particle, C is the specific heat of particles, M is the mass transmittance of a single particle under the influence of various factors, and $(\partial f/\partial t)_c$ is the collision integral term.

For the case of steady flow of homogeneous low-concentration solid particles, the collision term $(\partial f/\partial t)_c$ in equation (5) is small and negligible. Formula (5) can be simplified as

$$\frac{\partial f}{\partial t} + u_p^t \cdot \frac{\partial f}{\partial r} + \frac{f}{\partial u_p^t} \cdot (bf) = 0. \tag{6}$$

The equations of particle density conservation, momentum conservation, and kinetic energy conservation are as follows:

$$\delta n = \delta \int f \mathrm{d}u_p^t, \tag{7}$$

$$\delta \int m u_p^t f \mathrm{d}u_p^t = 0, \tag{8}$$

$$\delta \int \frac{1}{2} m u_p^2 f \mathrm{d}u_p^t = 0. \tag{9}$$

Under the condition of particle density conservation, momentum conservation, and kinetic energy conservation, it is not difficult to obtain the particle velocity distribution function by the variational method. According to the similar method of aerodynamic theory, a particle H function is defined as follows:

$$H = \int f \ln f \mathrm{d}u_p^t. \tag{10}$$

Because of equilibrium, we want H to have a minimum. Thus, the variational equation can be obtained:

$$\delta H = \delta \int f \ln f \mathrm{d}u_p^t. \tag{11}$$

Multiply the Lagrange operator $\lambda' (= \lambda + 1)$ by the scalar product of equations (7) and (8) and $(1/m)s$, and multiply equation (9) by another operator β to obtain

$$f = \exp\left(\lambda + s_i \cdot u_{pi}^t - \frac{1}{2} m\beta u_p^2\right) = A \exp\left(\lambda - \frac{1}{2} m\beta V^2\right). \tag{12}$$

We have

$$A = \exp\left[\frac{1}{2} m\beta\left(u_{o1}^2 + u_{o2}^2 + u_{o3}^2\right)\right], \tag{13}$$

$$\lambda = \int m\beta \vec{b}\,\mathrm{d}r = m\beta \int b_i \mathrm{d}r_i, \tag{14}$$

where s is the vector related to the instantaneous velocity u_p^t of particles, u_p^2 is the square value of particle characteristic velocity, and u_{pi} is the correlation characteristic velocity of particles.

For a simple two-dimensional flow, the unit mass force acting on particles in x and y directions can be expressed as

$$b_x = \frac{3}{4} \frac{C_D}{d_\rho} \frac{\rho_f}{\rho_p} \left|u_f^t - u_p^t\right| \left(u_{f1}^t - u_{p1}^t\right), \tag{15}$$

$$b_y = \frac{3}{4} \frac{C_1}{d_\rho} \frac{\rho_f}{\rho_p} \left(u_{f1}^t - u_{p1}^t\right)^2 - \left(1 - \frac{\rho_f}{\rho_p}\right) g, \tag{16}$$

where C_D is the resistance coefficient, C_1 is the lift coefficient, ρ_p is the material density of particles, and u_{f1}^t, u_{p1}^t are the fluid and the component of the instantaneous velocity of a particle in the x direction.

Through equations (12)–(16), the particle velocity distribution function can be obtained as follows:

$$f = A \exp\left\{m\beta\left[\frac{3}{4} C_1 \frac{\rho_f}{\rho_p}\left(u_{f1}^t - u_{p1}^t\right)^2 \frac{y}{d_p} - \left(1 - \frac{\rho_f}{\rho_p}\right) g y + C_1 + C_2\right] - \frac{1}{2} m\beta \sum \left(u_{f1}^t - u_{oi}\right)^2\right\}, \tag{17}$$

where C_1 and C_2 are determined by initial conditions and boundary conditions.

After the reverse circulation is formed in the cleaning tool tube, the fluid will interact with the debris particles. As long as the pressure inside the cleaning tool tube is

accelerated rapidly, the debris can gain upward velocity and enter the cleaning tool tube to complete the fishing operation.

2.1.2. Numerical Analysis. A wellbore cleaning tool structure based on jet negative pressure effect is shown in Figure 4, which mainly includes jet nipple, suction nipple, filter nipple, shunt nipple, one-way valve nipple, debris collection cylinder, bottom hole, and casing. The center of the top end is the origin of coordinates, the total length of the tool is 4200 mm, and the minimum inner diameter is 25 mm. In addition, Table 1 shows the dimensions and material parameters of each part of the cleaning tool. When the bottom hole debris is sucked into the cleaning tool under the reverse circulation formed by the tool section, the debris larger than the diameter of the screen is blocked when it reaches the filter nipple. After stopping the pump, it falls into the debris collection nipple under the action of the one-way valve. Finally, the lifting tool is salvaged.

In order to understand the fishing process of wellbore cleaning tools and the application of negative pressure effect in cleaning tools in detail, the flow passage of wellbore cleaning tools was extracted by using computational fluid dynamics (CFD) software, and fluent finite element model was established. The inlet is displacement and pressure boundary conditions. The outlet is the pressure boundary condition, and the pressure is the bottom hole pressure. In order to simulate the process of collecting cuttings at the bottom of the well, a certain volume of cuttings was present at the bottom of the well.

Figure 5 shows the salvage process of wellbore cleaning tools, which is divided into four stages: a, b, c, and d. In Figure 5(a), for the preparation stage, the debris is all deposited at the bottom of the wellbore. When the working fluid passes through the jet nipple and forms a reverse circulation in the tool section, the cuttings at the bottom of the well will enter the tool under the drive of the working fluid, as shown in Figure 5(b). Because there is less prepositioned debris at the bottom of the well, it is all sucked into the cleaning tool in a short time, as shown in Figure 5(c). When the debris continued to rise to the position of the screen tube, the movement of the debris stopped at the position of the screen tube because the diameter of the screen tube was smaller than the diameter of the debris, as shown in Figure 5(d). When the screen hole is completely blocked, turn off the high-pressure pump. Debris in the tool will fall from the screen into the debris collector by the action of a check valve. Finally, lift the tool to the surface to complete the salvage operation.

Therefore, the finite element method is used to verify that the wellbore cleaning tool based on negative pressure effect can establish local reverse circulation at the bottom of the well, drive the bottom debris into the cleaning tool, and stay in the tool to complete the salvage under the action of screen tube and one-way valve.

2.2. Salvage Experiment. To verify the salvage capability of the cleaning tool, the experiment bench shown in Figure 6(a) was established. The experiment process is as follows:

(a) Place the wellbore cleaning tool on the simulated wellbore experiment bed and connect it to the high-pressure pump

(b) Add abrasives to the simulated wellbore until the abrasives are marked

(c) Start the high-pressure pump, slowly boost the pressure to the specified pressure, synchronously start the camera for video collection until there is no abrasive inside the wellbore, record the time after abrasive removal, close the high-pressure pump, and then close the camera and stop the video, as shown in Figure 6(b)

(d) Set different pump pressures, repeat steps b and c, and finally get the results shown in Table 2

As can be seen from Figure 6(b), the whole test process is divided into four stages as follows:

(a) Preparation and suction stage: the main phenomenon is the disturbance of the high-pressure water jet to the bottom of the abrasive, so that the abrasive can obtain the initial velocity

(b) Initial entrainment phase: because of the entrainment of the fluid at the lower part of the tool near the nozzle outlet, the abrasive material with the initial velocity begins to move upwards with the fluid

(c) Suction process stage: when the whole system establishes a stable reverse circulation, when the fluid's force on the abrasive is greater than the abrasive's own weight, the abrasive will enter the tool along with the fluid to achieve the fishing effect

(d) End of roll: when all abrasives are involved in the inside of the tool, the salvage is complete

Table 2 shows four groups of test data and results. The results show that, with the increase of pump displacement, the suction speed is faster and the salvage efficiency of cleaning tools is higher.

Therefore, the test method verified the feasibility of the negative pressure cleaning tool. By means of the negative pressure generated by the high-pressure water jet and the entrainment of the high-speed water jet, reverse circulation is established in the negative pressure cleaning tool and the following parts to salvage the bottom debris.

3. Cleaning Tool Adaptability Analysis

3.1. Working Fluid Property. Different working fluids may produce different negative pressures near the nozzle when they pass through the jet stub, and the entrainment of the fluid near the nozzle by the high-pressure water jet may also be unnecessary. For example, the viscosity of different working fluids may be different and so may be the

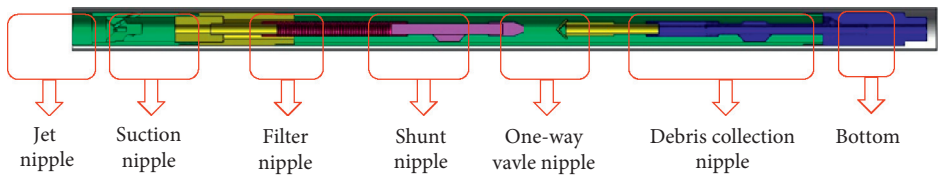

Figure 4: Cleaning tool structure.

Table 1: Dimensions and material parameters of cleaning tool.

Name	Length (mm)	Outer diameter (mm)	Inner diameter (mm)	Material	Elasticity modulus (GPa)
Jet nipple	113	80	16	42CrMo	210
Suction nipple	153	79	25	42CrMo	210
Filter nipple	528	46	35	45Steel	200
Shunt nipple	518	76	35	45Steel	200
One-way valve nipple	570	46	25	45Steel	200
Debris collection nipple	3000	104	96	42CrMo	210

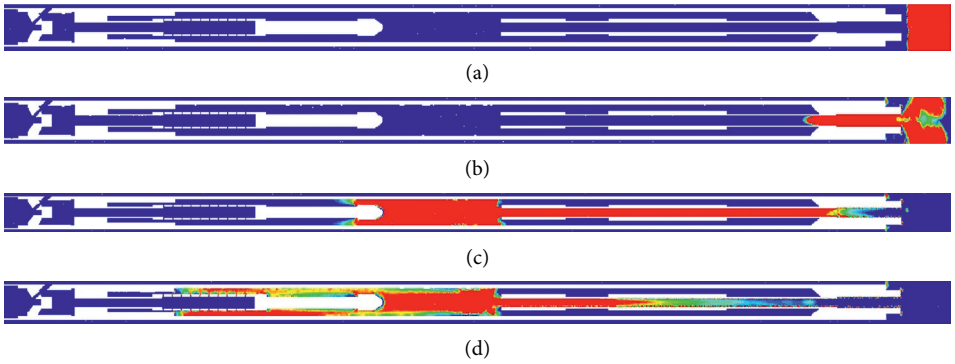

Figure 5: Salvage process of wellbore cleaning tools.

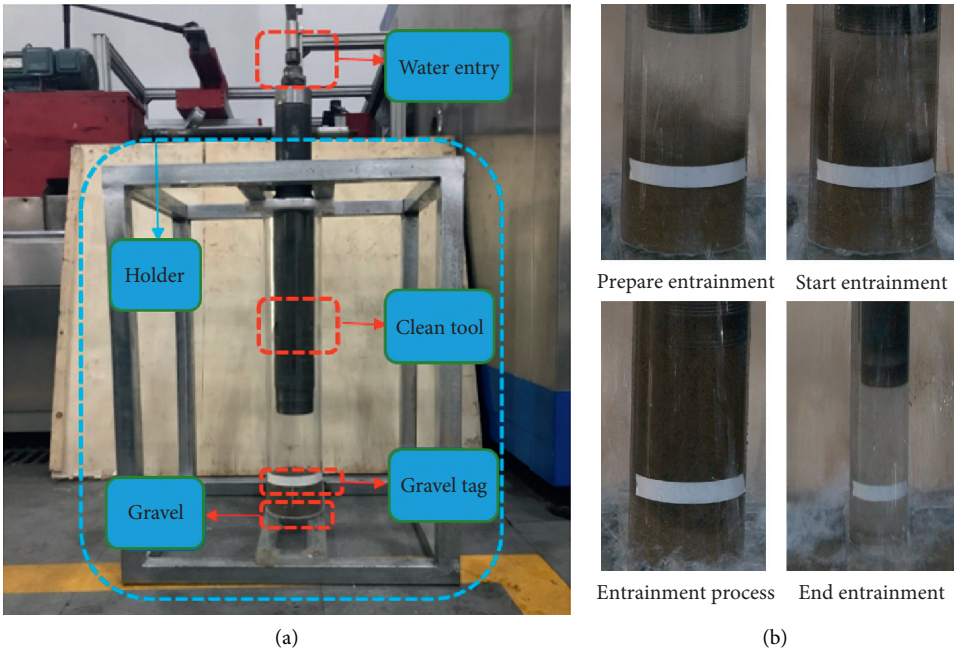

Figure 6: Cleaning tool salvage test. (a) Experiment bench. (b) Experiment process.

Table 2: Results of cleaning tools salvage under different inlet pressures.

Test number	The quality of abrasive (kg)	Pump displacement (L/min)	Inlet pressure (MPa)	End pumping time (s)	The remaining of sediment
1	1	91	5	34	Almost no
2	1	114	8	30	Almost no
3	1	128	10	25	Almost no
4	1	140	12	21	Almost no

disturbance to bottom hole debris and the migration of debris. Therefore, firstly, the influence of working fluid properties on the performance of wellbore cleaning tools is analyzed to find the appropriate working fluid.

As shown in Table 3, the density and viscosity parameters of different cases are given.

Figure 7 shows the global model of case 1 cleaning tool and the local static pressure results. In the global model (Figure 7(a)), it can be found that the inlet press0075re is the maximum, about 45.6 MPa. The inlet pressure of case 1 is set to 50 MPa, indicating a pressure drop of 4.4 MPa after the working fluid enters the tool. In addition, when the working fluid flows through the nozzle, the pressure significantly reduced. Since there are only three nozzles at the nozzle location, the area ratio of nozzle inlet to outlet is 23.38, and the flow rate of incompressible fluid at the inlet and outlet is the same; the velocity at the nozzle outlet is significantly higher than that at the inlet. According to Bernoulli's principle, the sum of kinetic energy and pressure potential energy is constant when the gravitational potential energy is not considered. Therefore, when the nozzle outlet kinetic energy is large, the pressure potential energy is bound to decrease.

As shown in Figure 7(b), the static pressure cloud diagram of nozzle position is given. The pressure is minimized at the edge of the nozzle outlet, and a local pressure gradient is formed at the nozzle outlet. This indicates that the high-speed fluid forms a low-pressure zone at the nozzle outlet, which results in the adsorption effect, that is, the negative pressure effect. Under the action of negative pressure effect, the pressure at the nozzle position is the least, and the pressure from top to bottom inside the cleaning tool gradually increases, as shown in Figure 7(c); for screen position, the pressure at the upper end is significantly lower than that at the lower end. As a result, a pressure gradient is formed in the cleaning tool tube to power the bottom hole detritus. Similarly, for bottom hole debris to enter the cleaning tool, the bottom of the tool should also have the adsorption of bottom hole debris. As shown in Figure 7(d), there is also a significant pressure difference at the bottom of the well.

In order to analyze the influence of working fluid properties on the fishing performance of cleaning tools, the calculation results of all cases in Table 3 are shown in Figure 8. Figures 8(a) and 8(b), respectively, show the pressure value and pressure difference at different positions of the cleaning tool at different working fluid density and viscosity. The position 0.26 m is the injection stub suction chamber and is regarded as the starting point of monitoring. The hole bottom is at 4.2 m. Obviously, the pressure value inside the cleaning tool increases from top to bottom, which is consistent with the result in Figure 7. Figure 8(a) shows that the higher the working fluid density, the lower the pressure value in the jet stub suction chamber. The reason is that the higher the density, the greater the kinetic energy of the high-pressure water jet, and the stronger the entrapment of the surrounding fluid under the Venturi effect. But, at the bottom of the well, the denser the fluid, the higher the pressure. This is because the working fluid flow at the bottom of the well is small. According to Bernoulli's principle, the higher the density of the fluid, the higher the pressure energy. Therefore, when the density is 1400 kg/m^3, the suction chamber pressure is the smallest and the bottom-hole pressure is the largest, and the pressure difference within the whole tool is the larger, as shown in Figure 8(b). Therefore, the appropriate increase of working fluid density is conducive to the improvement of cleaning tool performance.

Table 3: Parameters of different working fluids.

Case	Density (kg/m^3)	Viscosity (10^{-3} kg/m·s)
Cases 1–5	1000	1, 20, 40, 60, 80
Cases 6–9	1200	20, 40, 60, 80
Cases 10–13	1400	20, 40, 60, 80

The pressure gradient inside the cleaning tool determines the ability to lift up the debris at the bottom of the well, and the fluid flow speed determines the efficiency of the cleaning tool. Figures 9(a) and 9(b), respectively, show the fluid velocity of jet stub suction chamber and bottom hole location in operation with different working fluid properties. Obviously, the flow velocity of the jet stub suction chamber is obviously higher than that of the bottom hole. Because the fluid ejected from the jet nipple needs to be diverted from the annulus to the bottom of the well, the bottom hole velocity is low. With the increase of working fluid viscosity, the drilling fluid velocity decreases gradually, because the greater the viscosity of the fluid, the worse the flow performance of the fluid and the greater the energy loss in the flow process. However, the densest working fluid has the highest velocity and the highest fishing efficiency in the jet stub suction chamber and the bottom hole.

Therefore, when selecting the working fluid, under the condition that the formation pressure window is satisfied, the working fluid density should be appropriately increased to improve the pressure gradient inside the wellbore inclination tool, and the working fluid viscosity should be appropriately reduced to improve the fluid flow speed, thus improving the fishing ability and efficiency of the cleaning tool. In cases 1–13, case 10 is the most suitable for cleaning tool fishing; that is, the working fluid density is 1400 kg/m^3 and the viscosity is 0.002 kg/m·s.

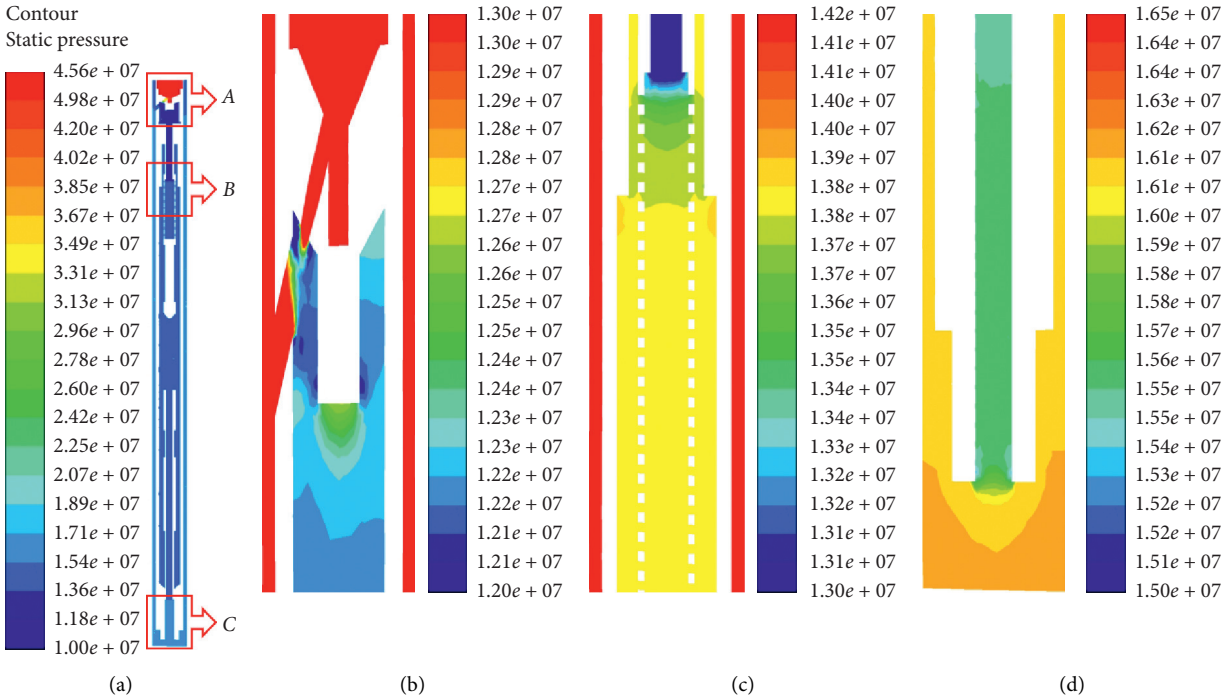

FIGURE 7: Static pressure results of case 1. (a) Global model. (b) Location *A*. (c) Location *B*. (d) Location *C*.

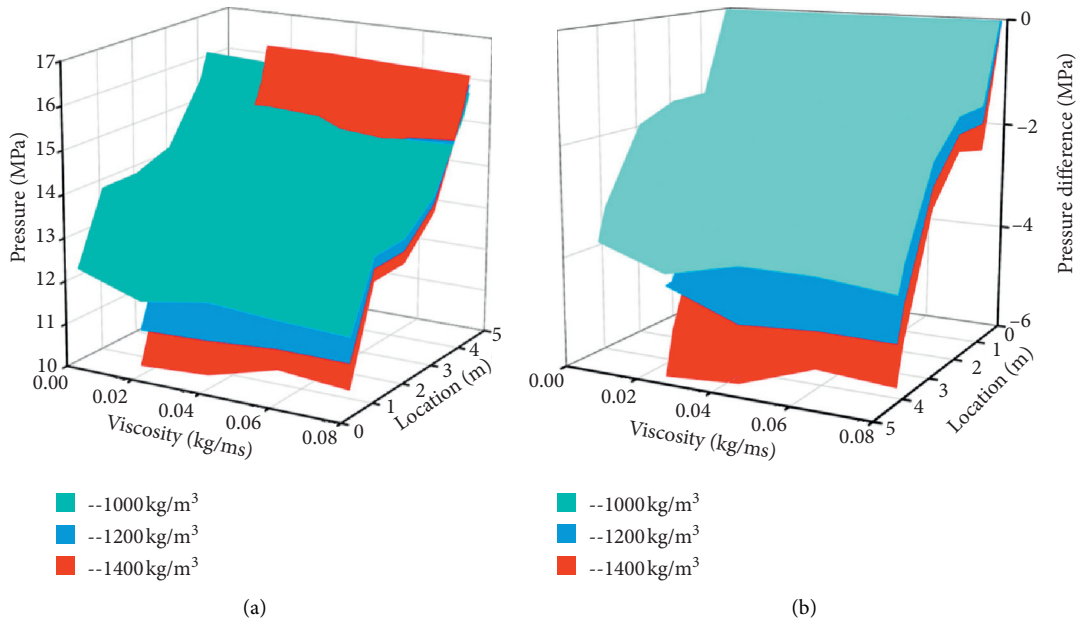

FIGURE 8: Influence of working fluid properties on cleaning performance. (a) Pressure; (b) differential pressure.

3.2. Sieve Tube Structure. Screen plays a crucial role in wellbore cleaning tools. If the screen hole is too small, it may affect the force of cleaning tools to pump bottom debris and easily cause screen blockage to be too fast. If the screen hole is too large, it cannot filter small particles, impacting the fishing effect. Therefore, it is necessary to analyze the structure of the screen tube and provide a basis for the selection of grinding shoes. In addition, with the advance of cleaning tools to salvage debris at the bottom of the well, the screen mouth is gradually blocked by debris, and the ability to absorb debris may gradually decrease. Therefore, it is necessary to analyze the screen blockage of the wellbore cleaning tool in the process of dredging debris, so as to provide a basis for the evaluation of the fishing ability of the cleaning tool and screen design.

Firstly, the size and distribution of screen diameter are analyzed. In order to ensure that the total area of screen tube flowing surface is the same, the case shown in Table 4 is

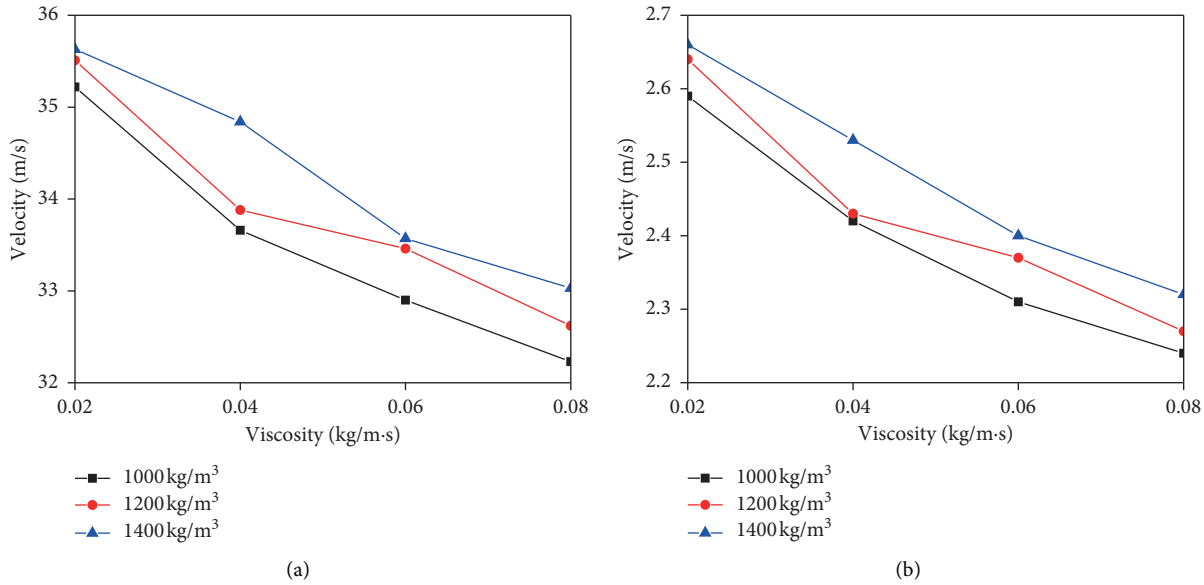

Figure 9: Influence of working fluid properties on fluid velocity. (a) Jet stub suction chamber; (b) bottom hole.

Table 4: Comparison of different screen diameters.

Case	Aperture (mm)	Number of axial distributions	Total area of screen hole (mm^2)
14	3	50	15795
15	4	37	
16	5	30	
17	6	25	

given. In all cases, the total flow surface area is 15795 mm^2, and the axial distribution numbers of apertures and holes are different, so as to analyze the influence of different structure of screen hole on cleaning tool performance.

Figure 10 shows the calculation results of cases 14–17, where Figure 10(a) shows the pressure difference between the jet stub suction cavity and different positions in different cases. The variation trend of pressure difference with tool location was basically the same in the four cases, and the pressure gradient with gradually decreasing pressure could be formed in the cleaning tool tube, indicating that reverse circulation could be formed at the bottom of the well in all cases to pump the bottom of the well debris. However, the negative pressure formed in case 16 is the largest, and the salvage ability for bottom hole debris is stronger. In order to better understand the influence of screen diameter on the size of negative pressure, Figure 10(a) also shows the variation law of pressure difference between the suction chamber and the bottom hole with the diameter. Obviously, when the diameter of the pipe is 5 mm, the negative pressure value is the largest; that is, case 16 is the most conducive to improving the fishing performance of cleaning tools.

Figure 10(b) shows the rate at which debris enters the cleaning tool in the case of screen with different diameters. The velocity increases first and then decreases with the size of the aperture, and the position of 5 mm aperture is the maximum point. Therefore, the combination of negative pressure and flow rate can obtain the maximum fishing capacity and maximum working efficiency of case 16, which is the optimal scheme for screen design. If the wellbore cleaning tool uses a 5 mm screen, the grinding shoes at the end of the string should also be selected.

In order to analyze the influence of screen blockage on cleaning tool performance, based on case 16, gradually reduce screen through-hole. When the cleaning tool is sucking debris, the upper flow rate of the screen tube is greater than the lower flow rate. The upper screen hole is usually blocked first in the operation process. Therefore, when reducing the screen tube hole, it is necessary to first close the screen tube top hole. Table 5 gives examples of different number of screen holes.

Figure 11 shows the velocity vector results of the fluid in cases 18–23 at the screen position. When the screen hole is less, the flow rate of through-hole position is faster. When the number of axial through-holes is large, the fluid velocity is higher at the upper through-hole than at the lower through-hole because the fluid enters the screen tube and turns inward. A very important conclusion is that, in all cases, the flow velocity at the top of the screen is basically the same, and the number of axial distribution holes in the screen has little effect on the fishing performance of the cleaning tool. As long as the total screen area is greater than 526.5 mm^2 during the operation, the wellbore cleaning tools can be salvaging normally.

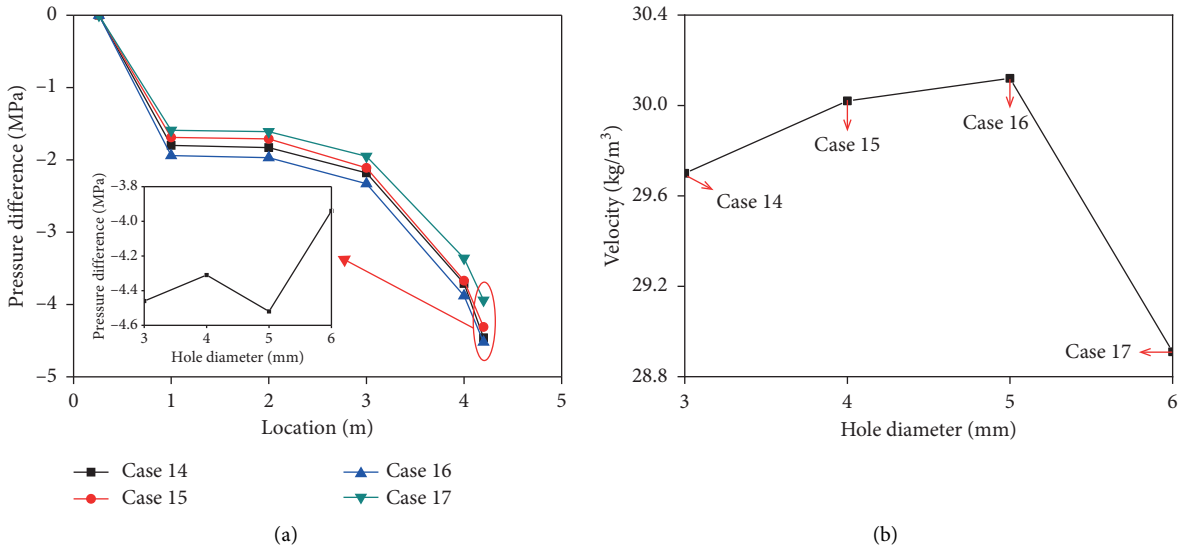

Figure 10: Influence of different screen diameters on cleaning performance. (a) Differential pressure; (b) speed.

Table 5: Cases of different through-hole numbers of screen tube.

Case	Aperture (mm)	Number of axial distributions	Total area of screen hole (mm^2)
18	5	1	526.5
19		3	1579.5
20		5	2632.5
21		10	5265
22		20	10530
23		30	15795

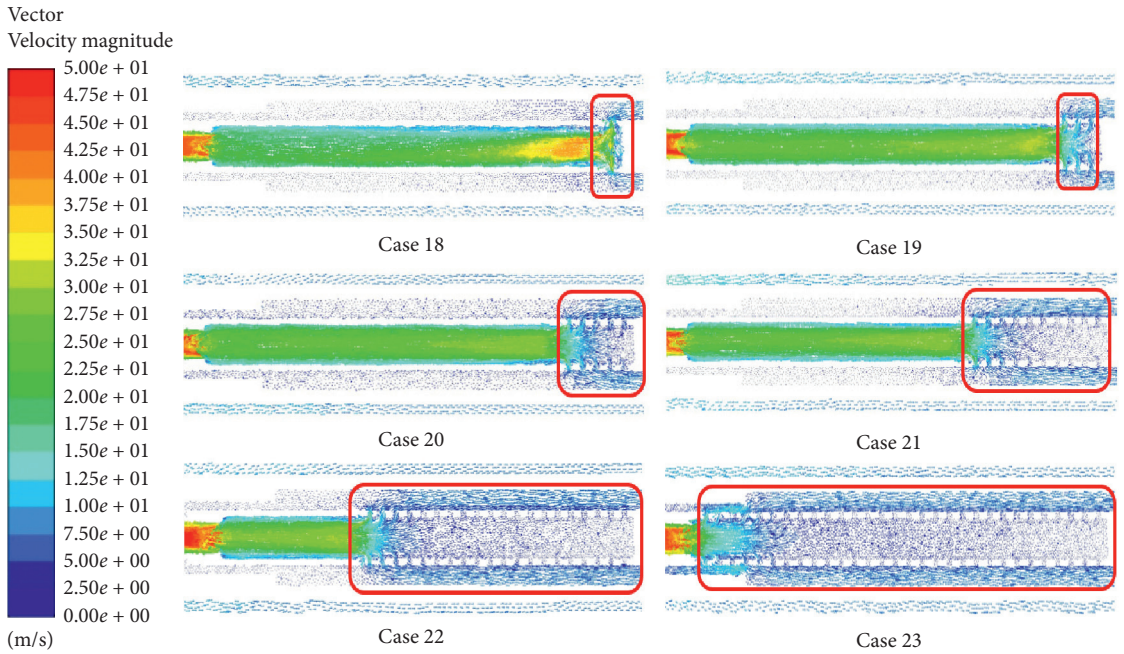

Figure 11: Influence of different mesh number on cleaning efficiency.

4. Operating Parameter Optimization

In addition to good structural design, wellbore cleaning tools also need to study reasonable operating parameters. It is very important to seek reasonable working parameters for field operation, which directly affects the fishing ability of cleaning tools. Therefore, it is necessary to study the main operating parameters to determine the optimal operating parameters of cylinder cleaning tool.

4.1. Inlet and Annulus Pressure. The wellbore cleaning tool is mainly affected by two pressure factors during operation, namely, the inlet pressure of the tool and the annular pressure. The inlet pressure is provided by the ground pump, while the annular pressure is controlled by the ground throttle manifold, so both pressure values can be adjusted within a certain range. Therefore, Table 6 gives 25 different cases to analyze the influence of inlet pressure and annulus pressure on cleaning tools to salvage bottom debris, providing guidance for surface pressure pump and throttle manifold control.

Figure 12 shows the influence law of different inlet pressure and annular pressure on pressure at different positions inside the tool. Figure 12(a) shows the changes of inlet pressure to the pressure at different locations of the cleaning tool when the annular pressure is different. With the increase of inlet pressure, the pressure in the inlet cavity of the jet stub decreases linearly but increases linearly at the bottom of the well. This is because the greater the inlet pressure, the greater the initial pressure energy provided by the cleaning tool and the greater the pressure drop formed when the high-pressure fluid passes through the nozzle. Because the high-pressure fluid is injected into the annulus through the jet nozzle, the flow impinges on the casing wall thickness, the flow velocity decreases, and the kinetic energy is converted into the potential energy of pressure, so the pressure at the bottom of the well increases linearly.

It can also be found in Figure 12(a) that the internal pressure of the cleaning tool increases as a whole when the annular pressure increases from 10 MPa to 18 MPa. According to Figure 12(b), the internal pressure of the cleaning tool increases linearly. Because the annular pressure is the pressure outlet of the wellbore cleaning tool system, the greater the pressure, the greater the obstruction to the fluid flow of the cleaning tool system.

As an important parameter in the evaluation of cleaning tools, the difference between injection nipple and bottom hole pressure directly affects the ability of cleaning tools to pump bottom hole debris. Therefore, Figures 13(a) and 13(b), respectively, show the influence of inlet pressure and annular pressure on the overall pressure difference of cleaning tools, and the slope is approximately −0.11 and 0.11, respectively. It indicates that the absolute value of the influences of inlet pressure and annular pressure on the overall differential pressure of cleaning tools are basically the same, but increasing inlet pressure is beneficial to improve the fishing performance of cleaning tools, while increasing outlet pressure reduces outlet pressure performance.

Table 6: Different inlet and annulus pressure cases.

Case	Inlet pressure (MPa)	Annulus pressure (MPa)
Cases 24–28	20	10 12 14 16 18
Cases 29–33	30	10 12 14 16 18
Cases 34–38	40	10 12 14 16 18
Cases 39–43	50	10 12 14 16 18
Cases 44–48	60	10 12 14 16 18

Therefore, in order to improve the fishing performance of wellbore cleaning tools, the annular pressure should be reduced through the throttle valve, so as to reduce the outlet pressure of cleaning tool system. In addition, the pump pressure can also be increased to increase the cleaning tool inlet pressure to improve the cleaning tool differential pressure. However, when the bottom hole pressure is increased, the safe density window of the wellbore should be considered to avoid or reduce the wellbore leakage accidents.

4.2. Displacement. Displacement, as another important parameter of pump, has a direct impact on cleaning tool performance. Therefore, according to the displacement of the pump used in the drilling field between 300 and 1000 L/min, in order to expand the research scope, the case shown in Table 7 was formulated.

Figure 14 shows the influence law of displacement on the internal pressure of cleaning tool and the pressure difference of different positions relative to jet stub suction chamber. Obviously, with the increase of displacement, the suction chamber pressure of jet stub gradually decreases, while the bottom hole pressure gradually increases, which is consistent with the increase of pump pressure. This is because when the displacement increases and the jet passage is constant, the flow rate will increase, which makes the negative pressure effect more significant and the pressure drop of the jet stub suction chamber more obvious. However, the bottom hole fluid is affected by the internal structure of the cleaning tool, and the increase of the flow rate cannot be proportional to the increase of the nozzle of the jet short joint. According to Bernoulli equation, the pressure P is in the first power relation, while the velocity is in the second power relation. When the velocity is disturbed, the bottom hole fluid pressure will increase, as shown in Figure 14(a). Figure 14(b) shows that increasing displacement can significantly increase the pressure difference inside the cleaning tool, and the pressure gradient increases nonlinearly with displacement.

In addition to improving the suction of the cleaning tool to the bottom of the well debris, increasing the displacement can also improve the cleaning efficiency. The effect of displacement on the fluid flow rate inside the cleaning tool is shown in Figure 15. Obviously, the increased displacement increases the velocity of the jet stub suction chamber. At the same time, after increasing the displacement, the fluid velocity ejected by jetting nipple increases, which increases the velocity at the bottom of the well, and the disturbance to the bottom of the well increases, which makes the initial velocity

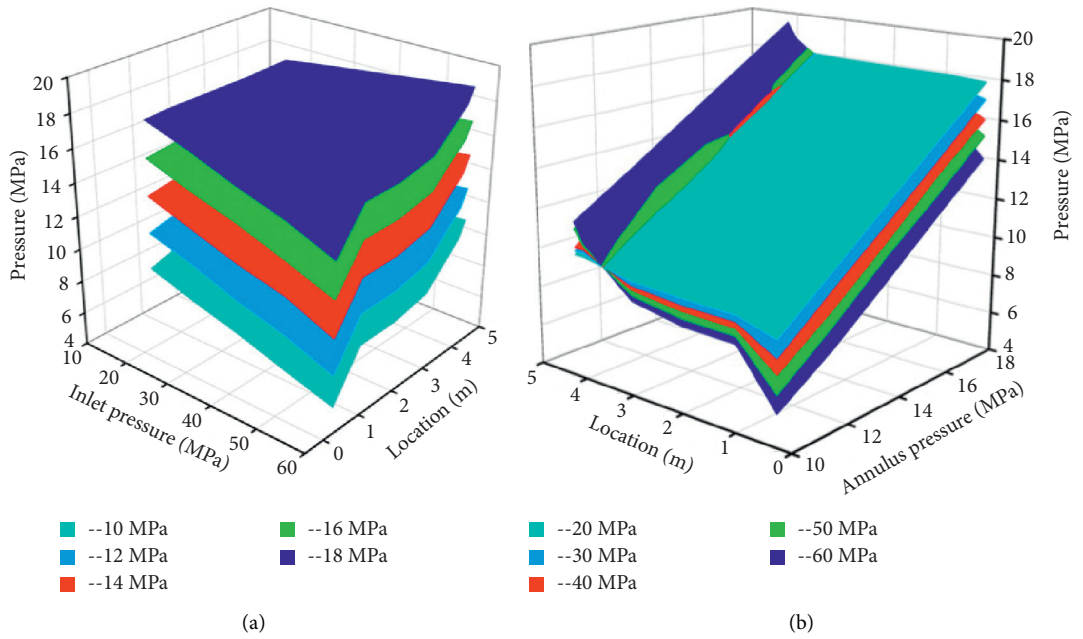

Figure 12: Influence of inlet pressure and annular pressure on tool internal pressure.

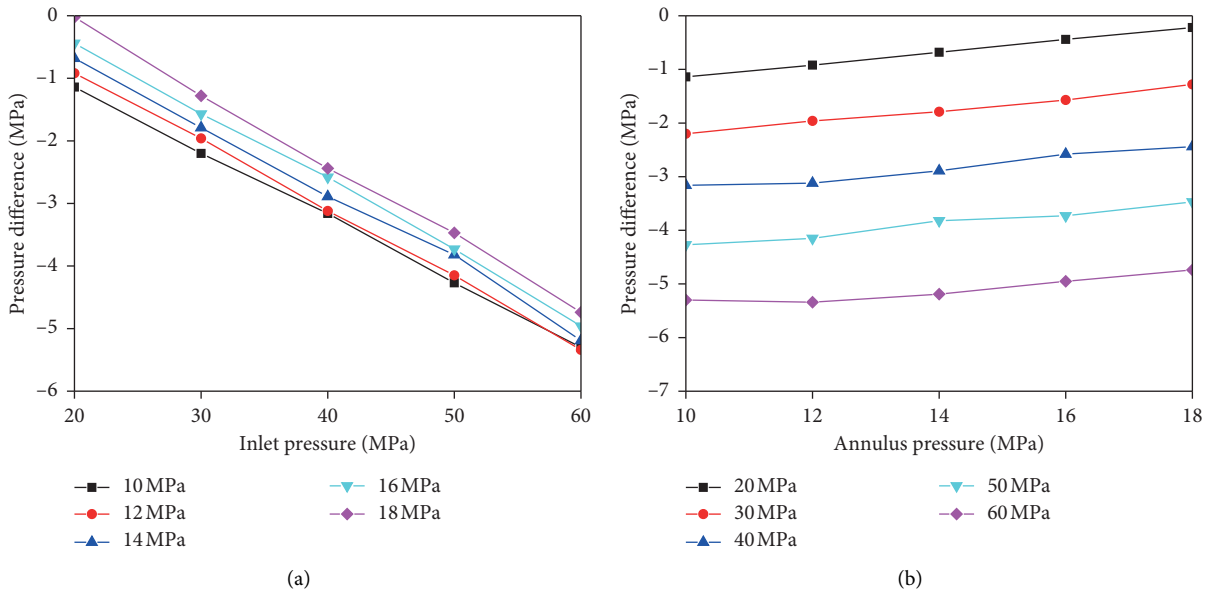

Figure 13: Influence of pressure on internal pressure gradient of cleaning tool. (a) Inlet pressure; (b) annular pressure.

Table 7: Different displacement cases.

Case	Displacement	Case	Displacement
Case 49	200	Case 52	800
Case 50	400	Case 53	1000
Case 51	600	Case 54	1500

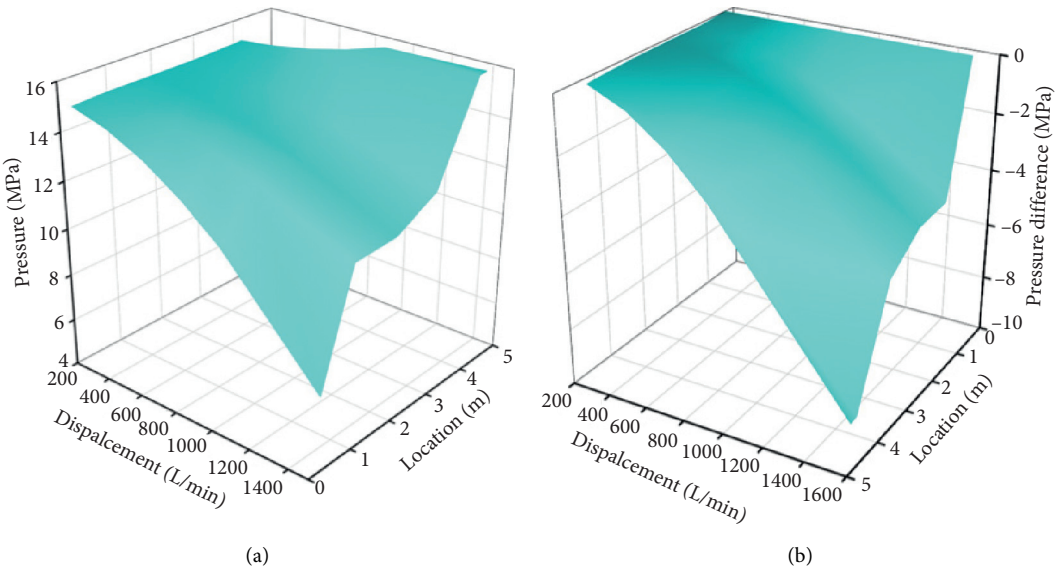

Figure 14: Effect of displacement on cleaning tool pressure.

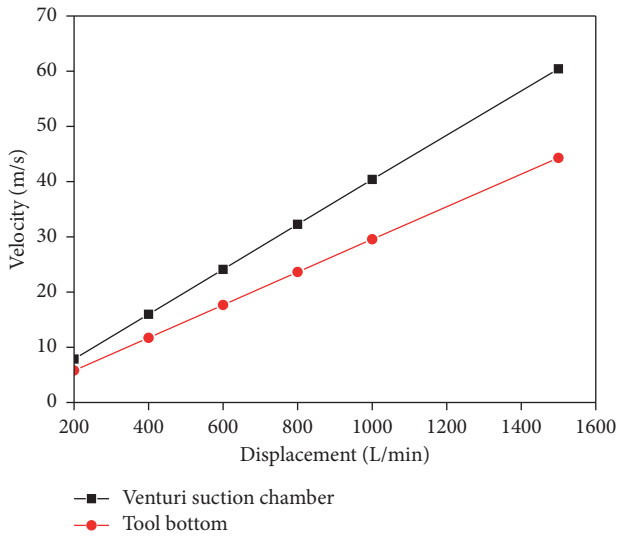

Figure 15: Influence of displacement on cleaning efficiency.

of the bottom of the well increase, which is more conducive to the mixing of the debris and working fluid into the cleaning tool tube. However, it should be noted that increasing the displacement will also increase the bottom hole pressure, so it is necessary to pay attention not to exceed the formation permeability pressure during the operation.

5. Conclusion

In order to solve the problem of detritus cleaning at the bottom of the well, this paper proposes a kind of wellbore cleaning tool to establish local reverse circulation at the bottom of the well based on the principle of negative jet pressure and liquid-solid two-phase flow theory. Through the analysis of the principle and influencing factors of cleaning tools, the following conclusions are obtained:

(1) A laboratory test was carried out on the jet stub to verify the feasibility of the negative pressure cleaning tool. At the same time, the finite element method was used to conduct the whole pipe modeling of the wellbore cleaning tool, and it was verified again that the wellbore cleaning tool based on the negative pressure effect could establish local reverse circulation at the bottom of the well, driving the bottom debris into the cleaning tool to complete the salvage.

(2) The influence of working fluid properties on cleaning tools was analyzed, and it was found that the increase of working fluid density was beneficial to improving the lifting ability of bottom hole debris, while the viscosity of working fluid would reduce the fishing efficiency of cleaning tools. High-density, low-viscosity working fluid can be selected on the premise of satisfying wellbore requirements. The cleaning tool has the maximum performance when the mesh aperture is 5 mm, and the net overflow area is not less than 526.5 mm^2, which will not affect the fishing performance of the cleaning tool.

(3) By analyzing the operating parameters of the cleaning tool, it is concluded that the wellbore annular pressure is the outlet boundary condition of the wellbore cleaning tool system. The increase of pump pressure and displacement is beneficial to improve the fishing performance and efficiency of cleaning tools. The pump pressure and displacement should be increased as far as possible on the premise of meeting the safety density window and the site.

Data Availability

The data used to support the findings of this study are included within the article.

Conflicts of Interest

The authors declare that they have no conflicts of interest.

Acknowledgments

This study was supported by the National Science and Technology Major Project (2017ZX05023-002) and Sichuan Science and Technology Program (2019YFG0305, 2018GZ0429, and 2018CC0098). The support is greatly appreciated by the authors.

References

[1] M. Cotton, I. Rattle, and J. Van Alstine, "Shale gas policy in the United Kingdom: an argumentative discourse analysis," *Energy Policy*, vol. 73, pp. 427–438, 2014.

[2] S. L. Montgomery, D. M. Jarvie, K. A. Bowker, and R. M. Pollastro, "Mississippian Barnett Shale, Fort Worth basin, north-central Texas: gas-shale play with multi-trillion cubic foot potential," *AAPG Bulletin*, vol. 89, no. 2, pp. 155–175, 2005.

[3] National Development and Reform Commission, *Energy Production and Consumption Revolutionary Strategy*, National Development and Reform Commission, Beijing, China, 2016.

[4] A. Mirani, M. Marongiu-Porcu, H. Y. Wang, and P. Enkababian, "Production-pressure-drawdown management for fractured horizontal wells in shale-gas formations," *SPE Reservoir Evaluation & Engineering*, vol. 21, no. 3, pp. 550–565, 2017.

[5] H. L. Zhang, S. Yang, D. M. Liu, Y. F. Li, W. Luo, and J. W. Li, "Wellbore cleaning technologies for shale-gas horizontal wells: difficulties and countermeasures," *Natural Gas Industry*, vol. 39, no. 8, pp. 82–87, 2019.

[6] T. Nazari, G. Hareland, and J. J. Azar, "Review of cuttings transport in directional well drilling: ystematic approach," in *Proceedings of SPE Western Regional Meeting*, pp. 1–15, Anaheim, CA, USA, May 2010.

[7] B. Bashir, "Review on hole cleaning for horizontal wells," *Journal of Engineering and Applied Sciences*, vol. 12, pp. 4697–4708, 2017.

[8] T. Xie, X. L. Ma, and J. Yuan, "Application of hydraulic thruster in drilling composite bridge plug in horizontal well," *China Petroleum Machinery*, vol. 45, no. 1, pp. 98–101, 2017.

[9] H. L. Zhang, G. S. Li, W. Wang, Z. W. Huang, and S. C. Tian, "Simplified model of critical fluid velocity for hole cleaning of horizontal well," *Drilling & Production Technology*, vol. 37, no. 4, pp. 5–8, 2014.

[10] J. Z. Zhao, Y. Peng, Y. M. Li, L. Wang, Y. Zhang, and Q. B. Mi, "Abnormal sand plug phenomenon at a high injection rate and relevant solutions," *Natural Gas Industry*, vol. 33, no. 4, pp. 56–60, 2013.

[11] M. E. Ozbayoglu, A. Saasen, M. Sorgun, and K. Svanes, "Hole cleaning performance of light-weight drilling fluids during horizontal underbalanced drilling," *Journal of Canadian Petroleum Technology*, vol. 49, no. 4, pp. 21–26, 2007.

[12] M. Duan, S. Z. Miska, M. Yu, N. E. Takach, R. M. Ahmed, and C. M. Zettner, "Critical conditions for effective sand-sized solids transport in horizontal and high-angle wells," *SPE Drill Completion*, vol. 24, no. 2, pp. 229–238, 2009.

[13] S.-M. Han, Y.-K. Hwang, N.-S. Woo, and Y.-J. Kim, "Solid-liquid hydrodynamics in a slim hole drilling annulus," *Journal of Petroleum Science and Engineering*, vol. 70, no. 3-4, pp. 308–319, 2010.

[14] Y. Tie, J. Y. Qu, X. F. Sun, and Z. J. Li, "Investigation on horizontal and deviated wellbore cleanout by hole cleaning device using CFD approach," *Energy Science and Engineering*, vol. 4, no. 7, pp. 1292–1305, 2019.

[15] X. J. Wang, L. Tang, and Z. Jiang, "Optimization of nozzle diameter and pressure drop of venturi ejector reactor based on numerical simulation," *Chemical Industry and Engineering*, vol. 32, no. 6, pp. 58–63, 2015.

[16] L. C. Wang, Y. Zhu, H. Zheng, and Q. Cai, "Simulation and analysis of the internal flow field for critical flow venturi nozzles based on Fluent," *Science Technology and Engineering*, vol. 13, no. 34, pp. 10392–10396, 2013.

[17] R. W. Paterson, "Turbofan mixer nozzle flow field-A Benchmark experimental study," *Journal of Engineering for Gas Turbines and Power*, vol. 106, no. 3, pp. 692–698, 1984.

[18] W. A. Eckerle, H. Sheibani, and J. Awad, "Measurement of the vortex development downstream of a lobed forced mixer," *Journal of Engineering for Gas Turbines and Power*, vol. 114, no. 1, pp. 63–71, 1992.

[19] S. Sundararaj and V. Selladurai, "Numerical and experimental study on jet trajectories and mixing behavior of venturi-jet mixer," *Journal of Fluids Engineering*, vol. 132, no. 10, pp. 101104–101112, 2010.

[20] B. J. Boersma, G. Brethouwer, and F. T. M. Nieuwstadt, "A numerical investigation on the effect of the inflow conditions on the self-similar region of a round jet," *Physics of Fluids*, vol. 10, no. 4, pp. 899–909, 1998.

[21] I. W. Eames, M. Worall, and S. Wu, "An experimental investigation into the integration of a jet-pump refrigeration cycle and a novel jet-spay thermal ice storage system," *Applied Thermal Engineering*, vol. 53, no. 2, pp. 285–290, 2013.

[22] C. Kanjanapon and A. Satha, "An experimental investigation of a steam ejector refrigerator: the analysis of the pressure profile along the ejector," *Applied Thermal Engineering*, vol. 24, no. 2-3, pp. 311–322, 2004.

[23] G. Raman and R. Taghavi, "Resonant interaction of a linear array of supersonic rectangular jets: an experimental study," *Journal of Fluid Mechanics*, vol. 309, pp. 93–111, 1996.

[24] S. H. Smith and M. G. Mungal, "Mixing, structure and scaling of the jet in crossflow," *Journal of Fluid Mechanics*, vol. 357, pp. 83–122, 1998.

[25] S. A. Sherif and R. H. Pletcher, "Jet-wake thermal characteristics of heated turbulent jets in crossflow," *Journal of Thermophysics and Heat Transfer*, vol. 5, no. 2, pp. 181–191, 1991.

[26] N. M. Said, H. Mhiri, G. L. Palec, and P. Bournot, "Experimental and numerical analysis of pollutant dispersion from a chimney," *Atmospheric Environment*, vol. 39, pp. 1727–1738, 2005.

[27] S. David, A. Zine, and O. Mohamed, "An experimental investigation of an ejector for validating numerical simulations," *Refrigeration*, vol. 34, no. 7, pp. 1717–1722, 2011.

[28] A. Ulas, "Passive flow control in liquid-propellant rocket engines with cavitating venturi," *Flow Measurement and Instrumentation*, vol. 17, no. 2, pp. 93–97, 2006.

[29] X. Lu, D. Wang, W. Shen, C. Zhu, and G. Qi, "Experimental investigation on liquid absorption of jet pump under operating limits," *Vacuum*, vol. 114, pp. 33–40, 2015.